

# Modeling of Liquid-Vapor Interfaces of Condensation Flows Based on Molecular Dynamics Simulations

Hiroki KANNAN, Susumu TERAMOTO, Toshio NAGASHIMA

Department of Aeronautics and Astronautics, School of Engineering, University of Tokyo  
7-3-1 Hongo, Bunkyo-ku, Tokyo, Japan  
kannan@thermo.t.u-tokyo.ac.jp

Keywords: Liquid-Vapor Interface, Condensation, Molecular Dynamics

## Abstract

Characteristics of a liquid-vapor interface where a nonequilibrium condensation flow exists are considered based on molecular dynamics simulations. The condensation coefficient, the velocity distributions of the reflected and evaporated molecules and the number flux of the evaporated molecules are compared with those under the liquid-vapor equilibrium.

The comparison shows that the condensation coefficient under the nonequilibrium condensation is slightly larger and the number flux of the evaporated molecules is considerably smaller than those under the liquid-vapor equilibrium.

The net condensation flux under the nonequilibrium condensation is underestimated if it is evaluated from the condensation coefficient and the number flux of the evaporated molecules under the liquid-vapor equilibrium. However the underestimation is relatively small.

## Introduction

Phase change at liquid-vapor interfaces is an important factor in the analysis of two phase flows related to propulsion systems. For example, cavitation, which is observed in turbopumps of liquid propellant rocket engines, is a phenomenon in which condensation and evaporation play an important role. In particular, significant nonequilibrium condensation occurs at liquid-vapor interfaces of collapsing cavitation bubbles, and physical properties inside the bubbles strongly depend on the phase change characteristics. In order to analyze such phenomena as bubble collapse, it is necessary to evaluate phase change fluxes exactly under liquid-vapor nonequilibrium conditions.

A thermal nonequilibrium field, for example vapor adjacent to a liquid surface called a Knudsen layer, is often treated based on kinetic theory of gasses<sup>1,2)</sup>. In the numerical analysis based on kinetic theory, boundary conditions at the liquid-vapor interface are vary important. They are a condensation coefficient (number ratio of condensed molecules to all molecules incident from vapor to the interface), velocity distributions of reflected and evaporated molecules and a number flux of evaporated molecules (hereinafter collectively called the interface characteristic).

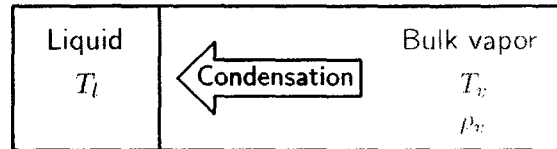


Fig. 1: Schematic view of the condensation condition

Among many studies<sup>3-7)</sup> on the interface characteristic, one of the typical examples is that by Tsuruta *et al.*<sup>8)</sup> They evaluated the interface characteristic of Argon under liquid-vapor equilibrium using molecular dynamics simulations. They assumed that the interface characteristic depends only on the temperature of the liquid surface, and applied the boundary conditions constructed from their molecular dynamics simulations to DSMC simulations of nonequilibrium phase change without any modification<sup>9)</sup>. Molecular dynamics simulations reported by Røsjorde *et al.*<sup>10,11)</sup> and Kjølstrup *et al.*<sup>12)</sup> support this assumption.

On the other hand, Chekmarev<sup>13)</sup> showed theoretically that a number flux of evaporated molecules is affected not only by liquid characteristics but also by vapor properties. Kotani *et al.*<sup>14)</sup> experimentally found that a condensation coefficient of methanol increases with increase of vapor temperature, and it decreases with increase of vapor density. Matsumoto<sup>15)</sup> reported similar results on Argon by molecular dynamics simulations. In this way, it is likely that the interface characteristic under the nonequilibrium phase change is different from that under the liquid-vapor equilibrium even when the temperature of the liquid surface is the same.

## Numerical Method

Numerical simulations under two conditions below are carried out for the discussion of the interface characteristic under nonequilibrium condensation.

**Condensation condition :** Non-equilibrium condensation as schematically shown in Fig.1.

**Equilibrium condition :** Liquid-vapor equilibrium at the same liquid surface temperature as the condensation condition.

Table 1: Input parameters. “[ ]” means a predicted value.

			Condensation condition	Equilibrium condition
Liquid surface temperature	$T_l$	(K)	102	[102]
Bulk vapor temperature	$T_v$	(K)	114	[102]
Bulk vapor number density	$\rho_v$	( $\text{m}^{-3}$ )	$8.03 \times 10^{26}$	$[3.67 \times 10^{26}]$
Saturation temperature	$T_{sat}$	(K)	—	102

Monoatomic molecules of Argon are treated as the most fundamental example. Input parameters are shown in Table 1.

The present study focuses on the difference in the interface characteristics between the condensation and equilibrium conditions.

### Molecular Dynamics Simulation

Molecular dynamics simulations are applied in order to follow up molecular motion directly.

Figure 3 shows simulation systems. The rectangular frames are the outer boundaries of the simulation domains. Each black point represents a center of a Argon molecule. High density regions on the left sides and the remaining low density regions correspond to the liquid and the vapor respectively. Hereinafter,  $x$  denotes the direction normal to the liquid-vapor interface, and  $y, z$  represent the parallel directions.

Each molecule moves based on the Newton’s law. The equations of motion are integrated using the velocity-Verlet method:

$$x^{n+1} = x^n + \Delta t u^n + \frac{\Delta t^2}{2m} f^n \quad (1)$$

$$u^{n+1} = u^n + \frac{\Delta t}{2m} (f^{n+1} + f^n) \quad (2)$$

where  $x^n$ ,  $u^n$  and  $f^n$  are a molecular position, velocity and intermolecular force at the  $n$ -th time step,  $\Delta t$  is the time interval and  $m$  is the mass of a Argon molecule. Intermolecular force is evaluated as a gradient of following Lennard-Jones(12-6) potential:

$$\phi(r) = 4\epsilon \left\{ \left( \frac{\sigma}{r} \right)^{12} - \left( \frac{\sigma}{r} \right)^6 \right\} \quad (3)$$

where  $\phi$  is intermolecular potential,  $r$  is a intermolecular distance and  $\sigma, \epsilon$  are potential parameters. The parameters are listed in Table 2.

### Boundary Condition

The simulation domain corresponds a part of liquid and vapor layers which are infinite in  $y$  and  $z$  directions shown in Fig.4.

In order to consider the molecules out of the simulation domain, counterparts of the simulation domain are laid out as shown in Fig.4. In the figure, the periodic boundary conditions are applied in  $y$  and  $z$  directions. In  $x$  direction, the counterparts are placed in the following way.

1. The simulation domain is displaced symmetrically to each side plane.
2. The displaced domain is moved in  $y$  and  $z$  directions by the half length of the simulation domain in order to prevent interaction between a molecule and its own counterparts.

Interaction between the molecules in the simulation domain and those in the counterparts is also taken into account.

### Adjustment of Temperature and Density

For the simulation of the condensation condition, three properties are adjusted to the target values shown in Table 1.

Two control regions are placed as shown in Fig.3. Temperatures of the blue and red regions are adjusted to the liquid surface temperature and the bulk vapor temperature respectively by the velocity-scaling method. That is, velocity of each molecule in a control region is modified using the following equation.

$$u' = \sqrt{\frac{T'}{T}} u \quad (4)$$

where  $u$  and  $u'$  are molecular velocities before and after the modification,  $T$  and  $T'$  are the temperature before the modification and the target temperature.

Density of the red region is fixed to the bulk vapor density as follows. When the density is lower than the target value, new molecules are added to the region at random, and the same number of molecules in the buffer region (the green region in Fig.3) are removed so that the liquid-vapor interface stay at the same location. When the density is higher, the opposite operation is carried out.

For the simulation of the equilibrium condition, temperature of the entire simulation domain is adjusted to the saturation temperature by the velocity-scaling method.

### Evaluation of Number Fluxes at the Liquid-Vapor Interface

Classification of condensed, reflected and evaporated molecules is necessary in order to evaluate the interface characteristic.

As shown in Fig.3, a reference plane is placed 2.0 (nm) apart from the plane where a density gradient is the maximum (hereinafter called “the maximum gradient plane”). This reference plane can

Table 2: Parameters of the molecular dynamics simulations

Time interval	$\Delta t$	(s)	$5.0 \times 10^{-15}$
Mass of a molecule	$m$	(kg)	$6.64 \times 10^{-26}$
Potential parameter	$\sigma$	(m)	$3.405 \times 10^{-10}$
	$\varepsilon$	(J)	$119.5 k_B$
Cut off distance	$r_c$	(m)	$3.5 \sigma$
Boltzmann constant	$k_B$	(J K <sup>-1</sup> )	$1.380658 \times 10^{-23}$

be regarded as the liquid-vapor interface for kinetic theory of gases.

Molecules passing the reference plane are marked as condensation, reflection or evaporation in the following manner.

**Condensation** : A molecule incident to the reference plane from the vapor, that arrives at the maximum gradient plane before it goes back to the vapor.

**Reflection** : An incident molecule that goes back to the vapor without arriving at the maximum gradient plane.

**Evaporation** : A condensed molecule that passes the reference plane from the liquid to the vapor.

## Results and Discussion

Figures 5 and 6 show the condensation coefficients, Figures 7 to 10 show the velocity distributions of the reflected and evaporated molecules, and Figure 11 shows the number fluxes of the condensed, reflected and evaporated molecules. In the figures, "Condensation" and "Equilibrium" indicate the results under the condensation and equilibrium conditions respectively.

The velocity distributions of the reflected and evaporated molecules are almost the same for two conditions, while the condensation coefficients and the number fluxes of the evaporated molecules are different.

These results are discussed in detail hereinafter.

### Difference in the Condensation Coefficients

Figures 5 and 6 show that

1. The condensation coefficient increases monotonously with the  $x$  velocity component of the incident molecule.
2. The condensation coefficient is independent of the  $y$  velocity component of the incident molecule.
3. The condensation coefficient under the condensation condition is slightly larger than that under the equilibrium condition.

The dependence of the condensation coefficient on the  $x$  velocity component of the incident molecule agrees with the result of Tsuruta's

simulations<sup>8)</sup> carried out under liquid-vapor equilibrium.

The difference in the condensation coefficients between two conditions can be explained as follows.

A molecule incident from the vapor to the reference plane collides with liquid molecules. Under the condensation condition, the liquid molecules have average velocity from the vapor to the liquid as shown in Fig.2, while they are stationary on average under the equilibrium condition. Therefore, average relative velocity between the incident vapor molecule and the liquid molecules under the condensation condition is smaller than that under the equilibrium condition, resulting lower collision probability and hence, the higher condensation coefficient.

### Difference in the Number Fluxes of the Evaporated Molecules

Figure 11 shows that the number flux of the evaporated molecules under the condensation condition is considerably smaller than that under the equilibrium condition.

Under the condensation condition, the vapor temperature and density are larger than those under the equilibrium condition. Therefore the probability that the molecules come out from the liquid collide with the vapor molecules and reflect back before they permeate the vapor, under the condensation condition is higher than that under the equilibrium condition.

### Net Condensation Flux

In most of the past studies based on kinetic theory of gasses, the condensation coefficient and the number flux of the evaporated molecules under the equilibrium condition are applied to the liquid-vapor interface under the condensation condition.

In order to estimate the error caused by this assumption, net condensation fluxes under the condensation condition evaluated based on the past method are compared with the present simulation result.

Hereinafter,  $\alpha$  and  $j$  denote a condensation coefficient and a number flux as functions of a  $x$  velocity component  $u_x$ , subscripts of "inc", "evap" and "net" represent all incident molecules, evaporated molecules and net condensation, and superscripts of "cond" and "eq" mean the condensation and equilibrium conditions.

When the condensation coefficient and the

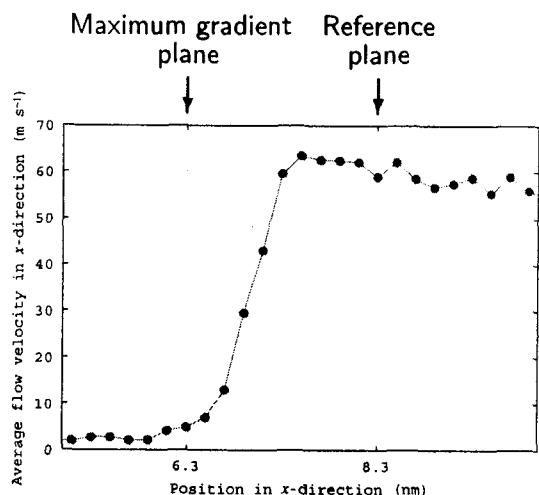


Fig. 2: Average flow velocity from the vapor to the liquid under the condensation condition

number flux of the evaporated molecules under the equilibrium condition are applied, the net condensation fluxes under the condensation condition are described as

$$j'_{\text{net}} = \int du_x \alpha^{\text{eq}} j_{\text{inc}}^{\text{cond}} - \int du_x j_{\text{evap}}^{\text{cond}} \quad (5)$$

$$j''_{\text{net}} = \int du_x \alpha^{\text{cond}} j_{\text{inc}}^{\text{cond}} - \int du_x j_{\text{evap}}^{\text{eq}} \quad (6)$$

respectively, supposing the number flux of all incident molecules is constant.

Results are shown in Fig.12. The middle bar shows the result of the molecular dynamics simulation for the condensation condition (same as the top of Fig.11). The red parts of the top and bottom bars represent  $j'_{\text{net}}$  and  $j''_{\text{net}}$ .

Figure 12 shows that the net condensation flux is underestimated by applying the condensation coefficient and the number flux of the evaporated molecules under the equilibrium condition. However, the difference of the condensation coefficients between two conditions is small, and the number flux of the evaporated molecules is much smaller than that of the condensed molecules under the condensation condition. Therefore the underestimation is relatively small.

### Summary

The number fluxes and the condensation coefficients at the liquid-vapor interface are evaluated using molecular dynamics simulations. Results under nonequilibrium condensation and the liquid-vapor equilibrium, are compared.

The comparison revealed that

1. The condensation coefficient under the nonequilibrium condensation is slightly larger and the number flux of the evaporated molecules is considerably smaller than those under the liquid-vapor equilibrium.

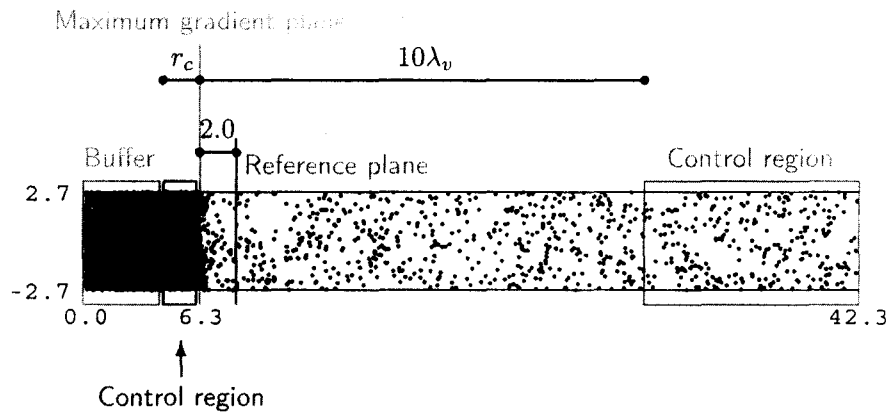
2. The net condensation flux is underestimated if it is evaluated based on the condensation coefficient and the number flux of the evaporated molecules which are evaluated from the equilibrium simulation. However the underestimation is relatively small.

### References

- 1) D. A. Labuntsov and A. P. Kryukov: Analysis of Intensive Evaporation and Condensation, *Int. J. Heat Mass Transfer*, **22**, 1979, pp.989-1002.
- 2) R. Meland and T. Ytrehus: Evaporation and Condensation Knudsen Layers for Nonunity Condensation Coefficient, *Phys. Fluids*, **15**(5), 2003, pp.1348-1350.
- 3) Yasuoka, K., Matsumoto, M. and Kataoka, Y.: Evaporation and Condensation at a Liquid Surface. I. Argon, *J. Chem. Phys.*, **101**(9), 1994, pp.7904-7911.
- 4) Matsumoto, M., Yasuoka, K. and Kataoka, Y.: Evaporation and Condensation at a Liquid Surface. II. Methanol, *J. Chem. Phys.*, **101**(9), 1994, pp.7912-7917.
- 5) Matsumoto, M.: Molecular Dynamics Simulation of Interphase Transport at Liquid Surfaces, *Fluid Phase Equilibria*, **125**, 1996, pp.195-203.
- 6) I. W. Eames, N. J. Marr and H. Sabir: The Evaporation Coefficient of Water: A Review. *Int. J. Heat Mass Transfer*, **40**(12), 1997, pp.2963-2973.
- 7) R. Marek and J. Straub: Analysis of the Evaporation Coefficient and the Condensation Coefficient of Water, *Int. J. Heat Mass Transfer*, **44**, 2001, pp.39-53.
- 8) Tsuruta, T., Tanaka, H. and Masuoka, T.: Condensation/evaporation coefficient and velocity distributions at liquid-vapor interface. *Int. J. Heat Mass Transfer*, **42**, 1999, pp.4107-4116.
- 9) Tsuruta, T. and Nagayama, G., DSMC Analysis of Interface Mass Transfer in Evaporation/Condensation Based on Molecular Dynamics Study, *Therm. Sci. Eng.*, **10**(1), 2002, pp.9-15.
- 10) A. Røsjorde, D. W. Fossomo, D. Bedeaux, S. Kjelstrup and B. Hafskjold: Nonequilibrium Molecular Dynamics Simulations of Steady-State Heat and Mass Transport in Condensation I. Local Equilibrium, *J. Colloid Interface Sci.*, **232**, 2000, pp.178-185.

- 11) A. Røsjorde, S. Kjelstrup, D. Bedeaux and B. Hafskjold: Nonequilibrium Molecular Dynamics Simulations of Steady-State Heat and Mass Transport in Condensation II. Transfer Coefficients, *J. Colloid Interface Sci.*, **240**, 2001, pp.355-364.
- 12) S. Kjelstrup, Tsuruta, T. and D. Bedeaux: The Inverted Temperature Profile Across a Vapor/Liquid Surface Analyzed by Molecular Computer Simulations, *J. Colloid Interface Sci.*, **256**, 2002, pp.451-461.
- 13) S. F. Chekmarev: Effect of Condensation Heat on the Condensation Coefficient, *AIChE J.*, **42(9)**, 1996, pp.2467-2475.
- 14) Kotani, M., Tsuzuyama, T., Fujii, Y., Fujikawa, S.: Nonequilibrium Vapor Condensation in Shock Tube, *JSME Int. J., B* **41(2)**, 1998, pp.436-440.
- 15) Matsumoto, M.: Molecular dynamics of fluid phase change, *Fluid Phase Equilibria*, **144**, 1998, pp.307-314.

(A) Condensation condition



(B) Equilibrium condition

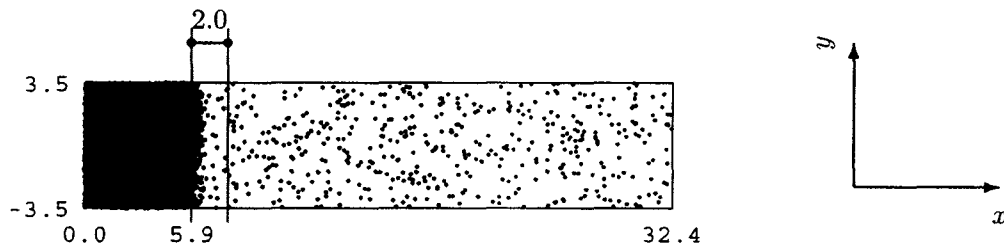


Fig. 3: The simulation systems. The unit of length is nm.

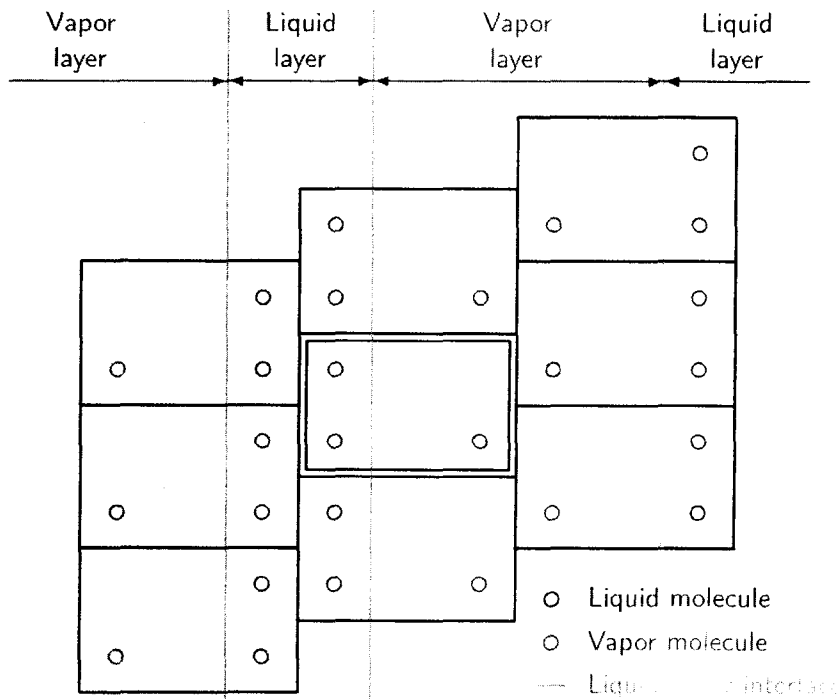


Fig. 4: Schematic view of the boundary condition. The center cell is the simulation domain, and the others are counterparts of the simulation domain.

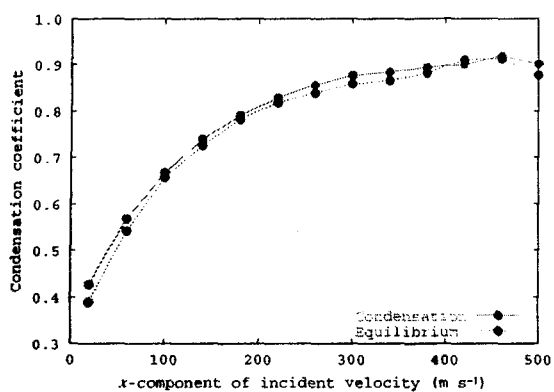


Fig. 5: Condensation coefficients for  $x$  velocity components of incident molecules

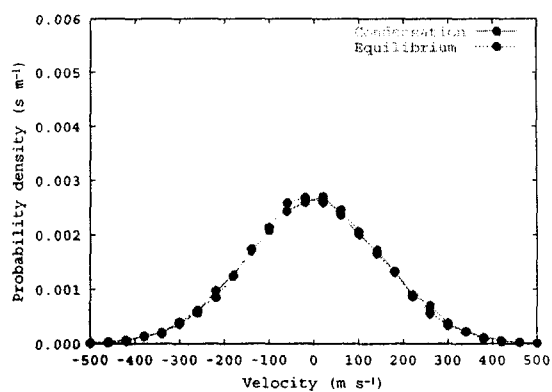


Fig. 8: Probability distribution of  $y$  velocity components of reflected molecules

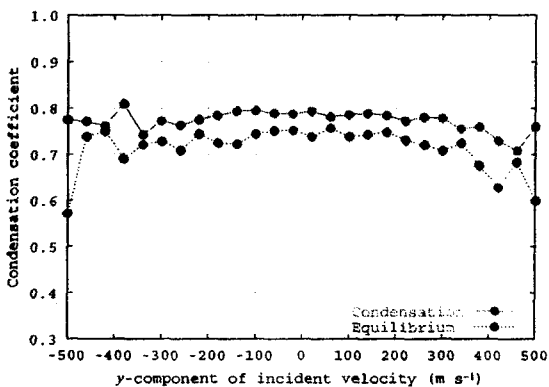


Fig. 6: Condensation coefficients for  $y$  velocity components of incident molecules

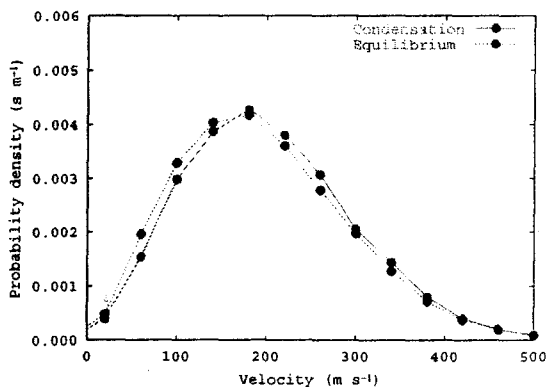


Fig. 9: Probability distribution of  $x$  velocity components of evaporated molecules

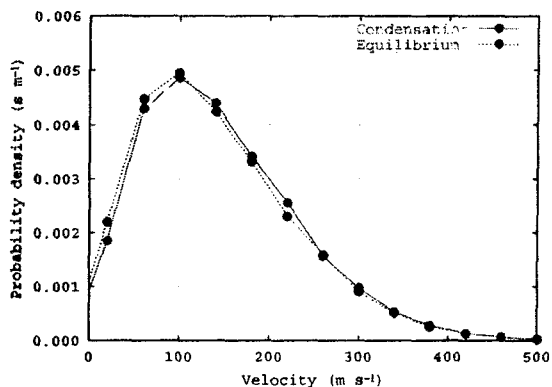


Fig. 7: Probability distribution of  $x$  velocity components of reflected molecules

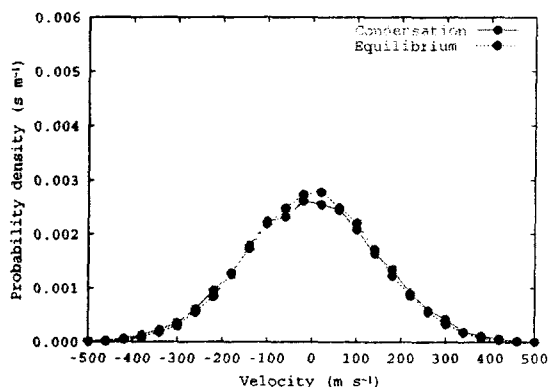


Fig. 10: Probability distribution of  $y$  velocity components of evaporated molecules

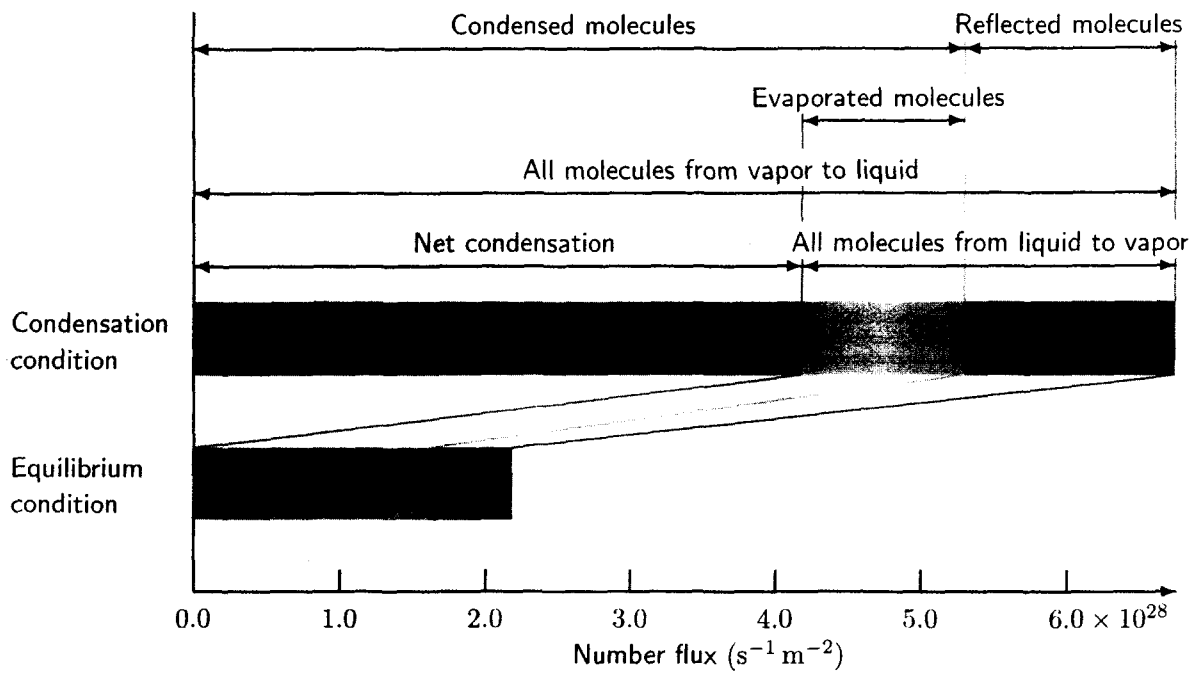


Fig. 11: Number fluxes of condensed, reflected and evaporated molecules.

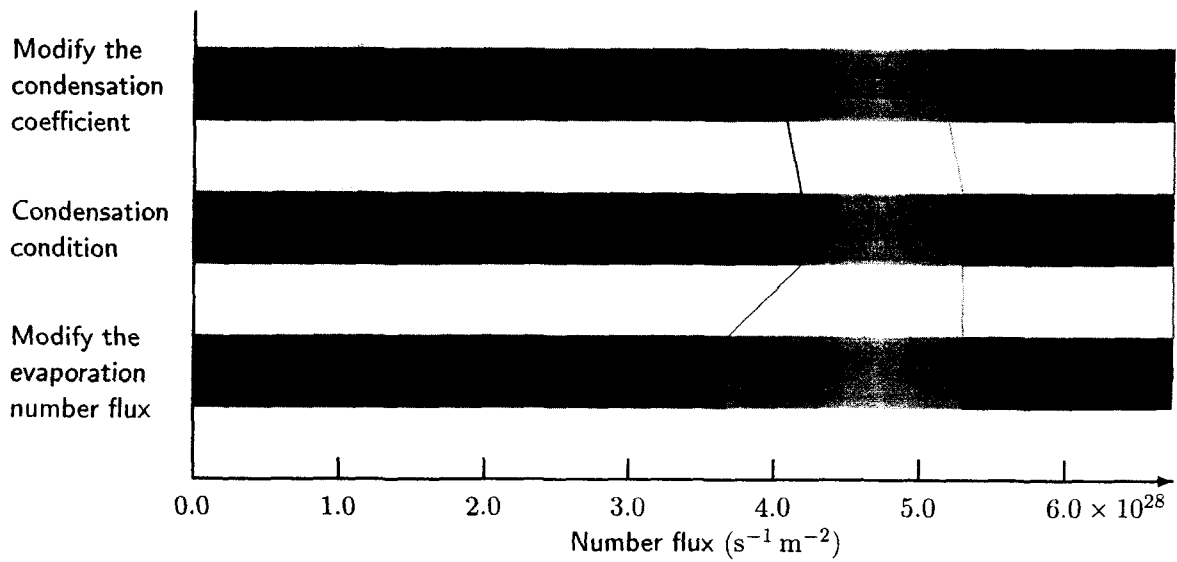


Fig. 12: Estimation of the net condensation flux under the condensation condition using the condensation coefficient and the number flux of the evaporated molecules under the equilibrium condition